Quantum 콘버어터의 모델링

정 규빈[0], 임 춘 택, 조 규 형

한국 과학 기술원 전기 및 전자공학과*

MODELING OF QUANTUM CONVERTERS

Gyu. B. Joung, Chun. T. Rim and Gyu. H. Cho

Department of Electrical Engineering Korea Advanced Institute of Science and Technology

ABSTRACT

Quantum converters, a subset of resonant converters operating with optimal conditions are modeled. It is shown that series resonant converter(SRC) can be modeled as buck/boost converter with an equivalent inductor and parallel resonant converter(PRC) can be modeled as Cuk converter with an equivalent capacitor. Also new resonant circuits with boost, buck-boost and Cuk converter characteristics are proposed. From these models, the quantum converters can be designed to be controlled with closed loop feedback, having many advantages such as low device switching stress, reliable high frequency operation and low EMI.

I. INTRODUCTION

PWM dc/dc converters are being replaced by resonant converters throughout the industry and aerospace applications because the filters and isolation transformers can be minized in size and weight[1-4]. In order to control the output voltage, frequency domain control scheme and phase domain control scheme[2] have been used, however, the device switching stresses become severe when the switching frequency deviates from the resonant frequency or the phase difference of the switches increases. Integral cycle mode control of SRC is reduces the switching stress and controls the output voltage[1]. In this method, discrete number of pulses(half cycles) of resonant frequency should be properly selected repeatedly by a proper feedback algorithm to control the output voltage.

In order to apply suitable feedback algorithm for closed loop control of output voltage, converter dynamics or converter modeling is very important. So far, state space modeling of general buck/boost switching power converters are well known. However, resonant converter modeling are complicated in general because of their nonlinear characteristics against load and switching frequency. Recently the model of the resonant converters has been studied[4], however, that kind of modeling is too complex to apply in the real situation.

In this paper, quantum converter which includes all kinds of resonant converters whose duty cycles are controlled with always integer multiple of resonant half period is modeled. It is named because the duty cycle is controlled discretely rather than continuously. It is shown that quantum SRC has buck/boost converter characteristics and quantum PRC has Cuk converter characteristics. A new quantum SRC with boost and buck-boost converter characteristics are also proposed, modeled and simulated. Quantum converters can be controlled to have nearly zero device switching loss, reliable high frequency operation and low EMI with variable output voltage by proper feedback algorithm, which are the distinctive features of the quantum converters.

II. MODELING OF THE QUANTUM CONVERTERS

A. Quantum Buck SRC

The power circuit topology of the SRC is shown in Fig. 1. When the SRC operates on optimal switching mode, that is, on/off of the switch pairs always occur in synchronization with the current zero crossing points, the output voltage can be controlled by the duty ratio of the powering mode and the free resonant mode as shown in Fig. 2, resulting in quantum buck SRC.

The switch modes of SRC can be approximately analyzed by low ripple approximation method[3] because the output filter capacitor C_o is sufficiently larger than the resonant capacitor C. In SRC, the output voltage v_o and the filter input current $|i_L(t)|$ are meaningful values. During the half resonant period $T/2$, the filter input current waveform is half sinusoidal as shown in Fig. 2. Because $C_o \gg C$ in practical, the more important state variables are $v_o(k)$ and $i_o(k)$:

$$i_o(k) = |i_{Lav}(k)| = \frac{2}{\pi}|i_p(k)|$$

where $i_p(k)$ is a peak resonant current, $i_{Lav}(k)$ is average resonant current and $v_o(k)$, $i_o(k)$ are output voltage and filter input current during the k-th resonant half period, respectively.

a. Powering mode :

Powering mode is defined when S1,S4 and S2,S3 pairs are turned on/off alternately in order to deliver power from source to load. During the k-th resonant period, resonant current $i_L(t)$ becomes

$$|i_L(t)| = v_c^*(k)+V_s-v_o(k)\sin(\omega_r t) \qquad (1)$$

where, $v_c^*(k)$ is the absolute value of tank capacitor voltage at the k-th switching instant and V_s is the source voltage.

Thus, the filter input average current of the k-th resonant period $i_o(k)$ becomes

$$i_o(k) = \frac{2}{\pi}\frac{v_c^*(k)+V_s-v_o(k)}{Z} \qquad (2)$$

where, $Z = \sqrt{L/C}$.

From eq. (1), $v_c^*(k+1)$ and $v_o(k+1)$ become

$$v_c^*(k+1) = v_c^*(k)-2v_o(k)+2V_s \qquad (3)$$

$$v_o(k+1) = \delta v_c^*(k)+(1-\delta-\delta^*)v_o(k)+\delta V_s \qquad (4)$$

where, $\delta=2(C/C_o)$ and $\delta^*=(\frac{\pi}{2})Q\delta$.

From eq(2),(3),(4) and on the condition that $1>>\delta^*$, the discrete state variables are

$$x(k+1)=\begin{bmatrix}1 & -\frac{4}{\pi Z}\\ \frac{\pi}{2}\delta Z & 1-\delta^*\end{bmatrix}x(k)+\begin{bmatrix}\frac{4}{\pi Z}\\ 0\end{bmatrix}V_s \quad (5)$$

where, $x(k)=[\ i_o(k)\ \ v_o(k)\ ]^T$.

If we let

$$\dot{x}(t)=\frac{x(k+1)-x(k)}{T/2} \quad \text{and} \quad x(t)=x(k)$$

where $x(t)=[\ v_o(t)\ \ v_o(t)\ ]^T$, then eq. (5) can be approximately rewritten as follows:

$$\dot{x}(t)=\begin{bmatrix}0 & -(\frac{2}{\pi})^2\frac{1}{L}\\ \frac{1}{C_o} & -\frac{1}{RC_o}\end{bmatrix}x(t)+\begin{bmatrix}(\frac{2}{\pi})^2\frac{1}{L}\\ 0\end{bmatrix}V_s \quad (6)$$

b. Free resonant mode :

Free resonant mode is defined when D2,S4 and D4,S2 pairs are turned on/off alternately. In this mode, the resonant circuit voltage v_s is equal to zero as shown in Fig. 2(a). Therefore, all of the conditions are equal to those of the powering mode except that V_s is replaced by 0. From eq.(6), the state equation is given as follows:

$$\dot{x}(t)=\begin{bmatrix}0 & -(\frac{2}{\pi})^2\frac{1}{L}\\ \frac{1}{C_o} & -\frac{1}{RC_o}\end{bmatrix}x(t) \quad (7)$$

From eq. (6),(7) and Fig. 3, we know that the SRC model is the same as the buck converter model. The equivalent circuit parameters of the SRC are obtained as follows :

$$L_B=(\frac{\pi}{2})^2L \quad (8\text{-a})$$

$$C_{oB}=C_o \quad (8\text{-b})$$

$$R_B=R \quad (8\text{-c})$$

Eq. (8) means that quantum buck SRC operates as a buck dc/dc converter with an inductor L_B having the duty ratio quantized by the resonant half period $T/2$ for PWM operation.

B. Quantum Boost SRC

The switching of SRC with boost characteristics is newly proposed as shown in Fig. 4 by adding an additional switch S5. When S1,S4 and S2,S3 pairs are turned on/off alternately in synchronization with the resonant current zero crossing points, the output voltage can be controlled by the bi-direction switch S5. This modeling procedures are similar to those of the quantum buck converter. The equivalent circuit parameters of the quantum boost converter are as follows :

$$L_B=(\frac{\pi}{2})^2L \quad (9\text{-a})$$

$$C_{oB}=C_o \quad (9\text{-b})$$

$$R_B=R \quad (9\text{-c})$$

From eq. (9) and Fig. 4, we know that quantum boost converter operates as a boost dc/dc converter with an equivalent inductor L_B.

C. Quantum Buck-Boost SRC

The switching of SRC with buck-boost characteristics is proposed as shown in Fig. 5. The modeling procedures are similar to those of the quantum buck converter. The equivalent circuit parameters are as follows :

$$L_B=(\frac{\pi}{2})^2L \quad (10\text{-a})$$

$$C_{oB}=C_o \quad (10\text{-b})$$

$$R_B=R \quad (10\text{-c})$$

From eq. (10) and Fig. 5, we know that the quantum buck-boost converter operates as a buck-boost dc/dc converter with an equivalent inductor L_B.

D. Quantum Cuk PRC

Typical power topology of the PRC with Cuk converter characteristics is shown in Fig. 6. When the PRC operates at optimal switching conditions, switch pairs are always turned on/off alternatively in synchronization with the voltage zero crossing points. The quantum Cuk converter is also modeled. The equivalent circuit parameters are as follows:

$$L_{1B}=L_1 \quad (11\text{-a})$$

$$L_{2B}=L_2 \quad (11\text{-b})$$

$$C_{oB}=(\frac{\pi}{2})^2C_o \quad (11\text{-c})$$

$$R_B=R \quad (11\text{-d})$$

From eq. (11) and Fig. 6, we know that quantum Cuk converter operates as a Cuk dc/dc converter with an equivalent capacitor C_{oB}.

III. CHARACTERISTICS OF THE QUANTUM CONVERTERS

A. The Quantum Operation of the Resonant Converter

The output voltage of the SRC can be controlled by proper selection of the three switch modes and the each mode should be changed at the resonant current zero crossing points. Thus, the mode selection intervals are discrete and the minimum period of this interval is the resonant half period $T/2$.

Fig. 7 shows the resonant circuit voltage v_s and the resonant current i_L of the quantum buck converter for the general control pattern. We can control the output voltage by varying this control pattern. When the duty ratio of the control pattern is given by the powering mode $m(T/2)$ of the total period $n(T/2)$, the dc transfer functions ($G_v=V_o/V_s$) are shown in Fig. 8(a). By applying the similar method for the other quantum converters, the dc transfer functions are obtained as shown in Fig. 8(b), (c) and (d). The output voltage levels are quantized by V_s/n and the number of quantized levels are n. Thus, in order to reduce the quantization level of the output voltage, the number of n should be increased, however, the resonant current ripple generally increases for increasing n. Therefore, the optimal control pattern for this converter needs some compromise between minimum ripple and minimum output voltage step. The output voltage ripple also depends on the control pattern period $n(T/2)$.

Fig. 9 shows the simulated comparision of quantum buck converter and modeled buck converter for varying δ(2C/Co) = 0.1,0.01 and 0.001. The output voltage of quantum buck converter $v_o(t)$ is nearly coincided with that of

modeled buck convreter $v_{OB}(t)$ except ripple components of $v_o(t)$. These ripple component decrease as δ decrease. The filter input current $i_o(t)$ some high frequency ripple components, however, average current are also coincided with modeled buck current $i_B(t)$ shown in Fig. 9.

The modeling results of the quantum converters suggested in this paper show that these models are simple and exact if $C_o \gg QC$ and the output voltage levels are quantized by the control pattern. The resonant circuit of the quantum SRC is modeled by replacing an equivalent inductor to the conventional buck/boost dc/dc converter and the resonant circuit of the quantum PRC is modeled by replacing an equivalent capacitor to the Cuk dc/dc converter.

Hence, the control becomes easy if suggested modeling is used because the PWM dc/dc converter control algorithm can be applied to these quantum converters. Switching operations of the quantum converters are always synchronized to the resonant current zero crossing points of SRC or the resonant voltage zero crossing points of PRC. Therefore, the device switching stress and switching loss are considerably low and the resonant converter can operate up to a high frequency. Thus, the magnetic filters and isolation transformers can be minimized in size and weight.

IV. CONCLUSION

The quantum converters are modeled and the modeling results are discussed. The quantum converter operates at optimal device operating conditions, that is, low device switching stress and fixed resonant frequency to the resonant tank circuit. The output voltage is controlled by proper selection of the switch modes. The SRC and PRC resonant circuits are modeled as general dc/dc switching power converters with an equivalent inductor or capacitor. The modeling is simple and exact if $C_o \gg QC$. New quantum converters with boost and buck-boost characteristics are also suggested and modeled. From these models, the output voltage of the quantum converters can be controlled by proper feedback algorithm, resulting in many advantage such as low switching loss, reliable high frequency operation, low EMI, etc.

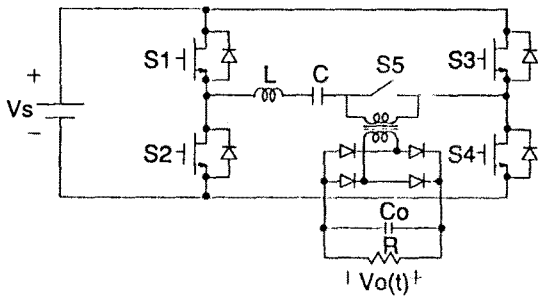

Fig. 1 Power circuit topology of SRC.

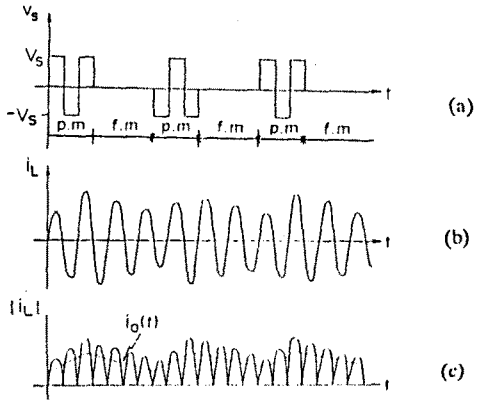

Fig. 2 Quantum buck converter waveforms (a) resonant circuit voltage v_r (b) resonant current i_L (c) filter input current $|i_L|$ and equivalent filter input current $i_o(t)$ where, p.m represents the powering mode and f.m represents free resonant mode.

buck converter	quantum buck converter
S : ON	S1,S4 S2,S3 pairs
S:OFF and D:ON	D2,S4 S2,D4 pairs

(a)

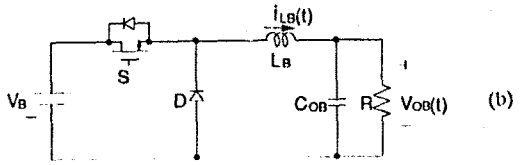

Fig. 3 Switching of SRC with buck converter characteristics (a) switching of the SRC shown in Fig. 1 (b) modeled buck converter.

boost converter	quantum boost converter
S : ON	S5 : ON
S:OFF and D:ON	S5 : OFF

(a)

*S1,S4 and S2,S3 pairs are always turned on and off alternately

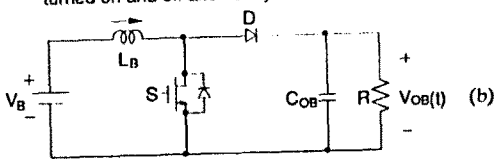

Fig. 4 Switching of SRC with boost converter characteristics (a) switching of the SRC shown in Fig. 1 (b) modeled boost converter

buck - boost converter	quantum buck boost converter
S : ON	S1,S4 S2,S3 pairs S5 : ON
S:OFF and D:ON	S2,D4 D2,S4 pairs S5 : OFF

(a)

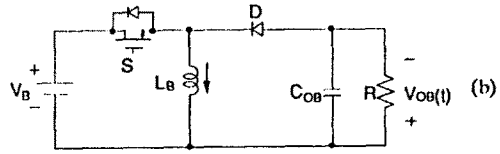

Fig. 5 Switching of SRC with buck-boost converter characteristics (a) switching of the SRC shown in Fig. 1 (b) modeled buck-boost converter

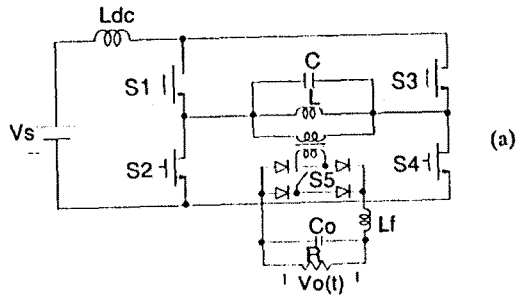

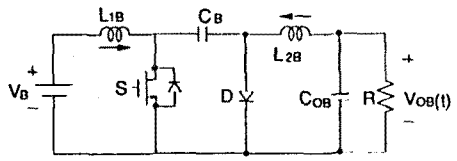

(b)

Cuk converter	quantum Cuk converter
S : ON	S1, S2 : ON S5 : OFF
S:OFF and D:ON	S1,S4 S2,S3 pairs S5 : ON

(c)

Fig. 6 PRC with Cuk converter characteristics (a) quantum Cuk converter (b) Cuk converter (c) switching of the converters

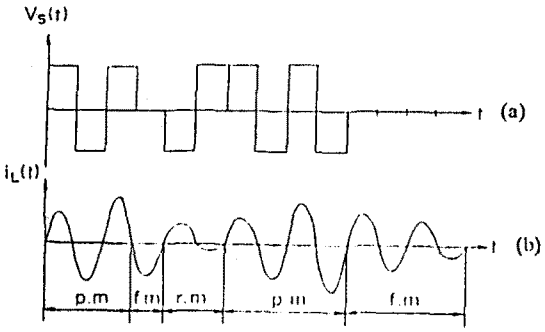

Fig. 7 Waveforms of the quantum buck converter for general control pattern, where p.m represents the powering mode, f.m represents the free resonant mode and r.m represents the regeneration mode.

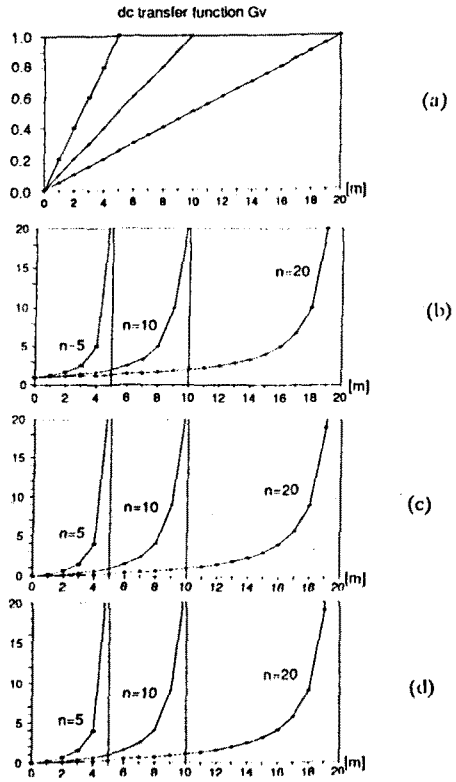

Fig. 8 Dc transfer function of the quantum converters (a) quantum buck converter (b) quantum boost converter (c) quantum buck-boost converter (d) quantum Cuk converter.

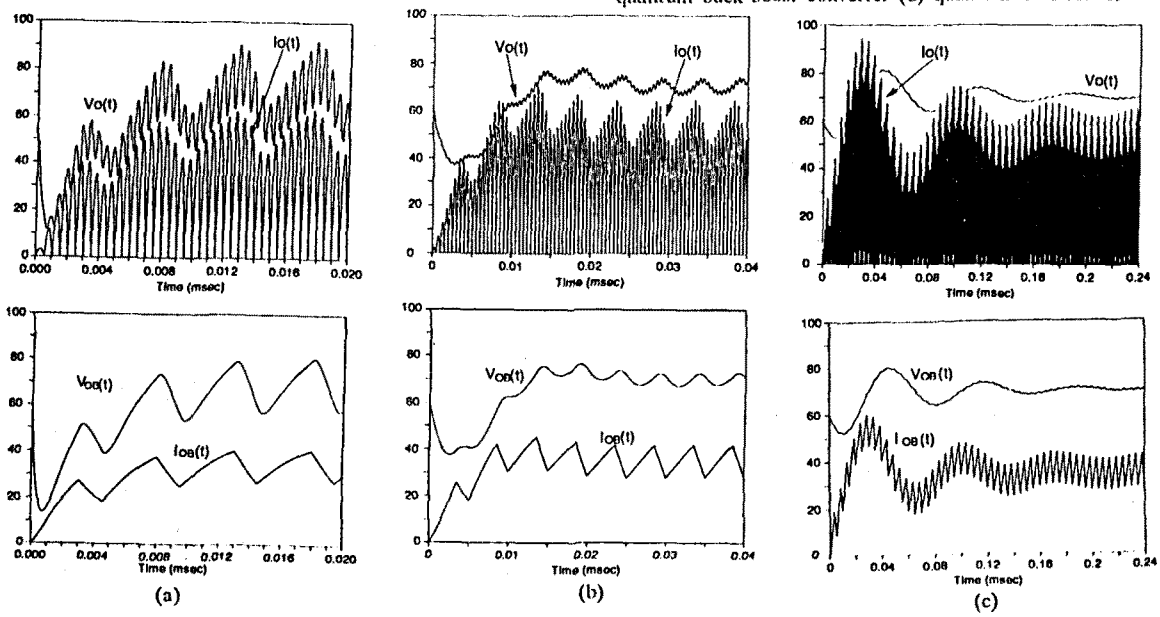

Fig. 9 Simulated comparision of quantum buck converter and modeled buck converter for varying δ. (a) δ=0.1 (b) δ=0.01 (c) δ=0.001 where, $V_s=100V$, $C=1600pF$, $L=16\mu H$, $V_o(0)=60V$, $i_o(0)=0A$.

REFERENCES

[1] G. B. Joung, C. T. Rim and G. H. Cho, " An integral cycle mode control of series resonant converter," IEEE PESC Rec., pp 575-682, 1988.

[2] Ira J. Pitel, "Phase-modulated resonant power conversion techniques for high frequency link inverters," IEEE Trans. Ind. Appl. vol. IA-22 , no. 6, pp.1044-1051, Nov. 1986.

[3] R. J. King and T. A. Sturat, "A large signal dynamic simulation for the series resonant converter," IEEE Trans. on Aerospace and Electronic Systems. Vol. AES-19. No. 6, pp. 859-870, Nov. 1983.

[4] Arthur F. Witulski and Robert W. Erickson, "Small signal ac equivalent circuit modeling of series resonant converter," IEEE PESC Rec., pp. 693-704, 1987.